FISEVIER

Contents lists available at ScienceDirect

Journal of Computational Physics

www.elsevier.com/locate/jcp



Bound/positivity preserving and unconditionally stable schemes for a class of fourth order nonlinear equations



Fukeng Huang a, Jie Shen b, Ke Wu b,*

- ^a Department of Mathematics, National University of Singapore, Singapore, 119076, Singapore
- ^b Department of Mathematics, Purdue University, West Lafayette, IN 47906, USA

ARTICLE INFO

Article history:
Received 31 December 2021
Received in revised form 23 March 2022
Accepted 26 March 2022
Available online 31 March 2022

Keywords: Bound/positivity preserving SAV approach Energy stability Fourth order equations Dissipative systems

ABSTRACT

We construct two classes of time discretization schemes for fourth order nonlinear equations by combining a function transform approach with the scalar auxiliary variable (SAV) approach. A suitable function transform ensures that the schemes are bound/positivity preserving, while the SAV approach enables us to construct unconditionally stable schemes. The first class of schemes requires solving a coupled second-order linear systems with variable coefficients at each time step, while the second class of schemes only requires solving a fourth-order linear equation with constant coeffcients. We apply this approach to the Cahn-Hilliard equations with logarithmic potential and the more challenging Lubrication-type equations, and present ample numerical examples to validate the accuracy and efficiency of the proposed schemes.

Published by Elsevier Inc.

1. Introduction

Solutions of many problems in science and engineering are required to be positive or within a prescribed interval. It is important, and oftentimes necessary, for a numerical method to preserve its bound/positivity. There exist a large literature on constructing positivity and/or bound preserving schemes for various problems, most of them are for first-order or second-order partial differential equations. In particular, for first-order hyperbolic systems, sophisticated post-processing (limiter) procedures for explicit schemes are developed in [27,26]. While the post-processing procedures can in principle be applied to explicit schemes for higher-order equations, there are not particularly efficient due to the severe time step constraints for explicit schemes to higher-order equations; For second-order parabolic systems, various numerical methods based on finite differences and finite elements have been developed by exploring the discrete maximum principle (see, for instance, [10–12,20,21] and the references therein).

On the other hand, less attention has been made to fourth- or higher-order systems with positivity and/or bound preserving properties. Two main difficulties for this class of problems are (i) the lack of maximum principle, and (ii) high-order spatial derivatives. Some existing approaches include:

• Cut-off and Lagrange multiplier approach: an ad-hoc approach is to simply cut off the values outside of the desired range. This approach is very simple and can achieve high order, under some specific situations, in L^2 -norm [23,19]. But

E-mail addresses: hfkeng@nus.edu.sg (F. Huang), shen7@purdue.edu (J. Shen), wu1589@purdue.edu (K. Wu).

This work is supported in part by AFOSR grant FA9550-20-1-0309 and NSF grant DMS-2012585.

^{*} Corresponding author.

drawbacks of this approach include: (i) difficult to conserve mass, and (ii) the solution obtained by the cut-off approach is usually not smooth so it is difficult to derive error estimates in energy norm.

- Convex splitting approach [3,7–9,15,22]: treat the convex part of the free energy implicitly to preserve bound/positivity, for examples, see [3] for Cahn-Hilliard equations with logarithmic potential. The drawback of this approach is that a nonlinear system has to be solved at each time step.
- Recently, a new Lagrange multiplier approach for constructing positivity preserving schemes was proposed in [5,6]. This approach includes the cut-off approach as a special case and provides a new interpretation for the cut-off approach. Furthermore, it can also preserve mass. But it is difficult to prove energy stability.

In [16], we combined the function transform with the SAV approach to construct unconditionally stable bound/positivity preserving schemes for second-order parabolic systems. The main idea was to use a suitable function transform so that the transformed function is always positive or within the specified bound, and then use the SAV approach to construct efficient unconditionally stable schemes for the transformed equation. This method was shown to be effective for a class of second-order equations in [16]. However, for fourth- or higher-order nonlinear systems, it appears that the transform systems can become very complicated and difficult to solve. The main purpose of this paper is to extend this approach to deal with fourth-order nonlinear systems.

To fix the idea, we consider the following fourth order nonlinear equations in a bounded domain $\Omega \subset \mathbb{R}^d$ (d=1,2,3):

$$\phi_t = \nabla \cdot (f(\phi) \nabla \mu),\tag{1.1a}$$

$$\mu := \frac{\delta E}{\delta \phi} = -\frac{1}{\alpha} \Delta \phi + H'(\phi), \tag{1.1b}$$

with either periodic or homogeneous Neumann boundary condition, where $f(\phi)$ is a positive mobility function, $H(\phi)$ is a nonlinear potential, and $E(\phi)$ is the free energy

$$E(\phi) = \int_{\Omega} \frac{1}{2\alpha} |\nabla \phi|^2 d\Omega + \int_{\Omega} H(\phi) d\Omega := E_0(\phi) + E_1(\phi). \tag{1.2}$$

An important feature of the above system is that the following energy dissipation law holds

$$\frac{dE}{dt} = -\int_{\Omega} f(\phi) |\nabla \mu|^2 d\Omega \le 0. \tag{1.3}$$

Examples of such equations include the Cahn-Hilliard equation [2], Lubrication-type equations [24]. In particular, with m > 0, we focus on the following two types of equations:

- Case 1. The Lubrication-type equations [24]: with $f(\phi) = m\phi^n$, n > 0 and $H(\phi) = 0$ in (1.1).
- Case 2. The Cahn-Hilliard equation with logarithmic potential [2,13]: with constant mobility $f(\phi) = m$ or variable mobility $f(\phi) = m\phi(1-\phi)$ in (1.1), and $H(\phi) = \phi\log\phi + (1-\phi)\log(1-\phi) + 3\phi(1-\phi)$ in (1.2).

We observe that for Lubrication-type equations, the values of solution ϕ have to be positive, while for the Cahn-Hilliard equation with logarithmic potential, the values of solution ϕ have to be within (0,1). The above two problems are challenging due to (i) the singular nonlinear mobility function, (ii) solutions need to be bound or positivity preserving, and (iii) fourth-order spatial derivatives.

We shall construct two classes of bound/positivity preserving and unconditionally stable schemes by combining the function transform approach and the SAV approach in [18,17]. For the first class, we rewrite the transformed equation as a system of two second-order equations, and then construct a class of linear and unconditionally stable schemes using the SAV approach. At each time step, it requires solving a linear system of two second-order equations with variable coefficients. This approach is most suitable for finite elements. It can also be used with a spectral discretization although it leads to coupled linear systems with non-sparse matrices. For the second class, we divide the transformed equation by T'(u), where $\phi = T(u)$ is a suitable function transform to guarantee positivity/bound preserving, and employ a suitable splitting of the nonlinear mobility function $f(\phi)$, so that after time discretization by the SAV approach with all nonlinear terms and terms with variable coefficients treated explicitly, one only needs to solve a system of two second-order linear equations with constant coefficients. This approach is particularly suitable for spectral discretizations (as well as for finite difference methods). The main contributions of this paper can be summarized as follows:

- We construct two classes of bound/positivity preserving schemes for two typical types of fourth order equations. These schemes are unconditionally stable and can achieve high-order accuracy in time.
- For both classes of schemes, we provide rigorous proofs for bound/positivity preserving and establish unconditional bounds for the numerical solutions.

• We combine these schemes with a time adaptive strategy, and carry out simulations of challenging problems to show their effectiveness and rubustness.

The rest of the paper is organized as follows. In the next section, we construct two classes of bound/positivity preserving schemes, and prove that they are unconditionally stable. In the third section, we present ample numerical examples to demonstrate the advantages of our numerical schemes. Some concluding remarks are given in the last section.

2. Bound/positivity preserving and unconditionally stable schemes

We present two methods to construct our bound/positivity preserving SAV for fourth-order equation: in the first method, we need to solve two coupled second-order equations with variable coefficients, which is most suitable for finite element method and can also be efficiently implemented with a preconditioned spectral discretization; in the second method, we only need to solve two coupled second-order equations with constant coefficients, which can be highly efficient by using a spectral or finite difference discretization.

Let $I = (0, \infty)$ or I = (0, 1) and assume that the values of solution ϕ are in I. Following the ideas in [16], which deals with the second order equations, we first make a suitable mapping $\phi = T(u)$ with the range of T in I, then the equation (1.1) on ϕ is transformed to an equation on u. Let u_h be an approximation to u, the range of the approximate solution $\phi_h = T(u_h)$ will always be in I. In particular, for two typical cases mentioned above, we can use the following transformations:

- $I = (0, \infty)$: a suitable choice is $T(v) = \exp(v)$, so that u = T(v) is always positive. I = (0, 1): suitable choices include $T(v) = \frac{1}{2} \tanh(v) + \frac{1}{2}$ or $T(v) = \frac{1}{1 + \exp(-v)}$, so that the range of u = T(v) is still in I.

Note that we have $T'(v) \neq 0$ for $v \in I$.

We assume that there exists constant $\underline{C} > 0$ such that

$$E_1(\phi) \ge -C + 1,\tag{2.1}$$

and we introduce a SAV $r(t) = E(\phi) + C_0$ with $C_0 = 2\underline{C} + \|E(\phi^0)\|_{L^{\infty}}$. Below, we shall describe two methods to solve the transformed equation for u.

2.1. Method 1

Setting $\phi = T(u)$ in (1.1), we can expand (1.1) by adding an equation for the SAV as follows:

$$T'(u)u_t = \nabla \cdot (f(\phi)\nabla\mu),$$
 (2.2a)

$$\mu = -\frac{1}{\alpha} \left(T'(u) \Delta u + T''(u) |\nabla u|^2 \right) + H'(\phi), \tag{2.2b}$$

$$\frac{dr}{dt} = -\frac{r}{E(\phi) + C_0} (f(\phi)\nabla\mu, \nabla\mu). \tag{2.2c}$$

Then given r^n and (u^j, ϕ^j) for $j = n, \dots, n-k+1$, we find $(\phi^{n+1}, u^{n+1}, r^{n+1}, \xi^{n+1})$ by the following scheme:

$$\begin{cases} T'(B_k(u^n)) \frac{\alpha_k \bar{u}^{n+1} - A_k(u^n)}{\delta t} = \nabla \cdot \left(f(B_k(\phi^n)) \nabla \bar{\mu}^{n+1} \right), \\ \bar{\mu}^{n+1} = -\frac{1}{\alpha} \left(T'(B_k(u^n)) \Delta \bar{u}^{n+1} + T''(B_k(u^n)) |\nabla B_k(u^n)|^2 \right) + H'(B_k(\phi^n)); \end{cases}$$
(2.3a)

If
$$I = (0, \infty)$$
: $\lambda^{n+1} = \frac{\int_{\Omega} \phi^0 dx}{\int_{\Omega} T(\bar{u}^{n+1}) dx}, \, \bar{\phi}^{n+1} = \lambda^{n+1} T(\bar{u}^{n+1}),$ (2.3b)

If
$$I = (0, 1)$$
:
$$\int_{\Omega} T(\lambda^{n+1} \bar{u}^{n+1}) dx = \int_{\Omega} \phi^0 dx, \ \bar{\phi}^{n+1} = T(\lambda^{n+1} \bar{u}^{n+1}), \tag{2.3c}$$

$$\frac{r^{n+1} - r^n}{\delta t} = -\frac{r^{n+1}}{E(\bar{\phi}^{n+1}) + C_0} \left(f(\bar{\phi}^{n+1}) \nabla \bar{\mu}^{n+1}, \nabla \bar{\mu}^{n+1} \right), \tag{2.3d}$$

$$\xi^{n+1} = \frac{r^{n+1}}{E(\bar{\phi}^{n+1}) + C_0}, \ \eta_k^{n+1} = 1 - (1 - \xi^{n+1})^{I_k}, I_k = \begin{cases} k+1, \ k \text{ odd} \\ k+2, \ k \text{ even} \end{cases},$$
 (2.3e)

$$u^{n+1} = \eta_k^{n+1} \bar{u}^{n+1}, \quad \phi^{n+1} = \eta_k^{n+1} \bar{\phi}^{n+1}, \tag{2.3f}$$

where the constant α_k , operators A_k , B_k are defined by

BDF1 scheme:

$$\alpha_1 = 1, \ A_1(v^n) = v^n, \ B_1(h^n) = h^n;$$
 (2.4)

BDF2 scheme: $\alpha_2 = \frac{3}{2}$, $A_2(v^n) = 2v^n - \frac{1}{2}v^{n-1}$, $B_2(h^n) = 2h^n - h^{n-1}$; (2.5)

BDF3 scheme:
$$\alpha_3 = \frac{11}{6}$$
, $A_3(v^n) = 3v^n - \frac{3}{2}v^{n-1} + \frac{1}{3}v^{n-2}$, $B_3(h^n) = 3h^n - 3h^{n-1} + h^{n-2}$; (2.6)

BDF4 scheme:
$$\alpha_4 = \frac{25}{12}$$
, $A_4(v^n) = 4v^n - 3v^{n-1} + \frac{4}{3}v^{n-2} - \frac{1}{4}v^{n-3}$, $B_4(h^n) = 4h^n - 6h^{n-1} + 4h^{n-2} - h^{n-3}$. (2.7)

The formulae for k = 5 and k = 6 can be derived similarly. Several remarks are in order:

- The mass conservation for $\bar{\phi}^{n+1}$ is guaranteed by (2.3b) or (2.3c), and the mass error for ϕ^{n+1} is $O(\delta t^{I_k})$. We can determine λ^{n+1} in (2.3b) explicitly for the positivity preserving case while we need to solve a nonlinear equation (2.3c) by iteration method to obtain λ^{n+1} for the bound preserving case.
- We choose I_k to be even and it satisfies $I_k \ge k+1$ to guarantee the whole scheme is k-th order accurate and $0 < \eta_k^{n+1} < 1$
- 1. As a result, the ranges of both $\bar{\phi}^{n+1}$ and ϕ^{n+1} are in I.

 (2.3d) is a first-order approximation to (2.2c). Hence, r^{n+1} is a first order approximation to $E(\phi(\cdot,t^{n+1}))+C_0$ which implies that ξ^{n+1} is a first order approximation to 1. Hence, $\eta_k^{n+1}=1+O(\delta t^{k+1})$, which implies that both $\bar{\phi}^{n+1}$ and ϕ^{n+1} are k-th order approximation of $\phi(t_{n+1}) = T(u(t_{n+1}))$.
- The above scheme can be efficiently implemented as follows:

 determine $(\bar{u}^{n+1}, \bar{\mu}^{n+1})$ by solving the coupled second-order system (2.3a);

 - compute $\bar{\phi}^{n+1}$ from (2.3b) or (2.3c); with $\bar{\phi}^{n+1}$ known, determine r^{n+1} explicitly from (2.3d), and compute ξ^{n+1} and η_k^{n+1} using (2.3e);
 - update ϕ^{n+1} and u^{n+1} using (2.3f), go to the next step.

Hence, the main computational cost is to solve the coupled second-order equations (2.3a) which amounts to solve the following coupled system:

$$a(\mathbf{x})u - \nabla \cdot b(\mathbf{x})\nabla v = f(\mathbf{x}), \tag{2.8a}$$

$$v + c(\mathbf{x})\Delta u = g(\mathbf{x}),\tag{2.8b}$$

where u and v satisfy either periodic or homogeneous Neumann boundary conditions, and a, b, c, f, g are given functions with a, b, c being positive.

Let X_h be a finite dimensional approximation space such that $X_h \in H^1(\Omega)$ if u and v satisfy the homogeneous Neumann boundary conditions, or $X_h \in H^1_p(\Omega) := \{v \in H^1(\Omega) : v \text{ periodic}\}\$ if u and v satisfy the periodic boundary conditions. And let $(\cdot,\cdot)_h$ be a discrete inner product on $X_h \times X_h$, a Galerkin approximation to (2.8) is: Find $u_h, v_h \in X_h$ such that

$$(a(\mathbf{x})u_h, \phi_h)_h + (b(\mathbf{x})\nabla v_h, \nabla \phi_h)_h = (f(\mathbf{x}), \phi_h)_h, \quad \forall \phi_h \in X_h, \tag{2.9a}$$

$$(v_h, \psi_h)_h - (\nabla u_h, \nabla (c(\mathbf{x})\psi_h))_h = (g(\mathbf{x}), \psi_h)_h, \quad \forall \psi_h \in X_h. \tag{2.9b}$$

Depending on the choice of X_h , the above coupled linear system can be solved directly or iteratively using a BiCGStab or GMRES with a suitable preconditioner.

Note that for this method, we need to solve a coupled second-order system with variable coefficients so it is mostly suitable if X_h consists of local basis functions such as finite-elements which would lead to a sparse system that can be efficiently solved. However, if X_h consists of global basis functions such as in a spectral method, it may lead to a non-sparse system that might be costly to form and solve. Hence, we shall present below a second method which is more suitable for a spectral discretization.

2.2. Method 2

Setting $\phi = T(u)$ in (1.1), introducing $v = \frac{\mu}{T'(u)}$ and dividing T'(u) on both sides, we can rewrite (1.1) as follows:

$$u_t - f(\phi)\Delta v = \frac{g(u, \phi, v)}{T'(u)},\tag{2.10a}$$

$$\nu + \frac{1}{\alpha} \Delta u = -\frac{T''(u)}{T'(u)} |\nabla u|^2 + \frac{H'(\phi)}{T'(u)},\tag{2.10b}$$

where $g(u, \phi, \nu)$ is given by

$$g(u,\phi,\nu) = f(\phi)(\nu\Delta T'(u) + 2\nabla\nu \cdot \nabla T'(u)) + \nabla f(\phi) \cdot \nabla\mu. \tag{2.11}$$

The transformed equation (2.10) is complicated. However, if $f(\phi)$ is a constant, the left hand side of (2.10) has only constant coefficients while the right hand side only has terms with lower-order derivatives. Thus, if we treat the left hand side implicitly and the right hand side explicitly, we only need to solve a system of linear equations with constant coefficients at each time step. Furthermore, in certain situations such as Cahn-Hilliard equations with logarithmic potentials, the nonlinear terms can be greatly simplified by choosing a suitable transform function.

To deal with the variable mobility, similar to the method presented in [30,1], we rewrite (2.10a) as

$$u_t - S_1 \Delta \nu + S_2 u = \tilde{g}(u, \phi, \nu) := \frac{g(u, \phi, \nu)}{T'(u)} + (f(\phi) - S_1) \Delta \nu + S_2 u, \tag{2.12}$$

where S_1 , S_2 are suitable positive constants.

We introduce a SAV $r(t) = E(\phi) + C_0$ with $C_0 = 2\underline{C} + ||E(\phi^0)||_{L^{\infty}}$ and rewrite (2.10) and (1.3) as

$$u_t - S_1 \Delta v + S_2 u = \tilde{g}(u, \phi, v), \tag{2.13a}$$

$$\nu + \frac{1}{\alpha} \Delta u = -\frac{T''(u)}{T'(u)} |\nabla u|^2 + \frac{H'(\phi)}{T'(u)},\tag{2.13b}$$

$$\phi = T(u), \quad \mu = T'(u)v, \tag{2.13c}$$

$$\frac{dr}{dt} = -\frac{r}{E(\phi) + C_0} (f(\phi)\nabla\mu, \nabla\mu). \tag{2.13d}$$

With $r(0) = E(\phi)|_{t=0} + C_0$, it is clear that the above system is equivalent to (1.1) with energy dissipative law (1.3).

Instead of discretizing (1.1), we shall discretize the expanded system (2.13) by using the general strategy introduced in [16] as follows:

Given r^n and (u^j, ϕ^j) for $j = n, \dots, n-k+1$, find $(\phi^{n+1}, u^{n+1}, r^{n+1}, \xi^{n+1})$ such that

$$\begin{cases}
\frac{\alpha_{k}\bar{u}^{n+1} - A_{k}(u^{n})}{\delta t} - S_{1}\Delta\bar{v}^{n+1} + S_{2}\bar{u}^{n+1} &= \tilde{g}\left(B_{k}(u^{n}), B_{k}(\phi^{n}), B_{k}(\bar{v}^{n})\right), \\
\bar{v}^{n+1} + \frac{1}{\alpha}\Delta\bar{u}^{n+1} &= -\frac{T''(B_{k}(u^{n}))}{T'(B_{k}(u^{n}))}|\nabla B_{k}(u^{n})|^{2} + \frac{H'(B_{k}(\phi^{n}))}{T'(B_{k}(u^{n}))},
\end{cases} (2.14a)$$

If
$$I = (0, \infty)$$
: $\lambda^{n+1} = \frac{\int_{\Omega} \phi^0 dx}{\int_{\Omega} T(\bar{u}^{n+1}) dx}, \ \bar{\phi}^{n+1} = \lambda^{n+1} T(\bar{u}^{n+1}),$ (2.14b)

If
$$I = (0, 1)$$
: $\int_{\Omega} T(\lambda^{n+1}\bar{u}^{n+1})dx = \int_{\Omega} \phi^0 dx$, $\bar{\phi}^{n+1} = T(\lambda^{n+1}\bar{u}^{n+1})$, (2.14c)

$$\bar{\mu}^{n+1} = \bar{\nu}^{n+1} T'(\bar{u}^{n+1}),$$
 (2.14d)

$$\frac{r^{n+1} - r^n}{\delta t} = -\frac{r^{n+1}}{E(\bar{\phi}^{n+1}) + C_0} \left(f(\bar{\phi}^{n+1}) \nabla \bar{\mu}^{n+1}, \nabla \bar{\mu}^{n+1} \right), \tag{2.14e}$$

$$\xi^{n+1} = \frac{r^{n+1}}{E(\bar{\phi}^{n+1}) + C_0}, \ \eta_k^{n+1} = 1 - (1 - \xi^{n+1})^{I_k}, I_k = \begin{cases} k+1, \ k \text{ odd} \\ k+2, \ k \text{ even} \end{cases}, \tag{2.14f}$$

$$u^{n+1} = \eta_{\nu}^{n+1} \bar{u}^{n+1}, \quad \phi^{n+1} = \eta_{\nu}^{n+1} \bar{\phi}^{n+1}, \tag{2.14g}$$

where the constant α_k , operators A_k , B_k are as before.

We observe that the main difference with Method 1 is that (2.3a) is replaced by (2.14a) which is now a coupled secondorder equation with constant coefficients and can be solved more efficiently, particularly with a spectral method or finite difference method.

2.3. A stability result

It is obvious that the schemes (2.3) and (2.14) are bound/positivity preserving. Moreover, we have also the following stability results.

Theorem 1. Given ϕ^i with range in I=(0,1) or $I=(0,\infty)$, $u^i=T^{-1}(\phi^i)$ for $i=0,1,\ldots,k-1$ and r^n . The schemes (2.3) and (2.14) admit a unique solution satisfying the following properties unconditionally:

- 1. Mass conservation for $\bar{\phi}^{n+1}$: $\int_{\Omega} \bar{\phi}^{n+1} dx = \int_{\Omega} \phi^0 dx$.
- 2. Bound preserving: i.e., the range of $\bar{\phi}^{n+1}$ and ϕ^{n+1} are in I.

3. Energy dissipation: Given $r^n > 0$ we have $r^{n+1} > 0$, $\xi^{n+1} > 0$ and

$$r^{n+1} - r^n = -\delta t \xi^{n+1} \left(f(\bar{\phi}^{n+1}) \nabla \bar{\mu}^{n+1}, \nabla \bar{\mu}^{n+1} \right) \le 0. \tag{2.15}$$

4. Furthermore, for the k-th order schemes, there exists $M_k > 0$ such that

$$\|\nabla \phi^n\| \le M_k, \, \forall n. \tag{2.16}$$

Proof. Eliminating $\bar{\nu}^{n+1}$ from (2.14a), we find that \bar{u}^{n+1} is the solution of

$$\left(\frac{\alpha_k}{\delta t} + S_2\right)u + \frac{S_1}{\alpha}\Delta^2 u = g,\tag{2.17}$$

subjected to the periodic boundary condition or $\frac{\partial u}{\partial n}|_{\partial\Omega}=\frac{\partial\Delta u}{\partial n}|_{\partial\Omega}=0$, and with g being a given function. It is clear that (2.17) admits a unique solution. On the other hand, (2.3a) leads to (2.8). It can be shown, using the standard theory for linear elliptic equations, that (2.8) with the periodic boundary condition or homogeneous Neumann boundary condition admits a unique solution.

The rest of the proof for the two schemes are exactly the same so we shall only do it for the scheme (2.14). It is obviously that the range of $\bar{\phi}^{n+1}$ is in I and $\int_{\Omega} \bar{\phi}^{n+1} dx = \int_{\Omega} \phi^0 dx$ from (2.14c).

We derive from (2.14e) that

$$r^{n+1} = r^n / \left(1 + \frac{\delta t}{E(\bar{\phi}^{n+1}) + C_0} \left(f(\bar{\phi}^{n+1}) \nabla \bar{\mu}^{n+1}, \nabla \bar{\mu}^{n+1} \right) \right).$$

Hence, if $r^n \ge 0$, we have $r^{n+1} \ge 0$, and (2.15) follows directly from (2.14e).

It follows from (2.14f), (2.15) and the definition of C_0 that

$$0 < \xi^{n+1} \le \frac{r^0}{E(\bar{\phi}^{n+1}) + C_0} < \frac{2|E(\phi^0)| + 2\underline{C}}{1 + |E(\phi^0)| + \underline{C}} < 2 \tag{2.18}$$

As a result, (2.14f) and (2.18) together imply

$$0 < (1 - \xi^{n+1})^{l_k} < 1, \ 0 < \eta_k^{n+1} < 1. \tag{2.19}$$

Hence, the range of ϕ^{n+1} is also in I as $\phi^{n+1} = \eta_{\nu}^{n+1} \bar{\phi}^{n+1}$.

Now, it follows from (2.14f) and the assumption on $E_1(u)$ that

$$|\xi^{n+1}| = \frac{r^{n+1}}{E(\bar{\phi}^{n+1}) + C_0} \le \frac{2r^0}{\|\nabla \bar{\phi}^{n+1}\|^2 + 2}.$$
(2.20)

Since $\eta_k^{n+1} = 1 - (1 - \xi^{n+1})^{I_k}$, there exists a polynomial P_k of degree $I_k - 1$ and a constant $M_k > 0$ such that

$$|\eta_k^{n+1}| = |\xi^{n+1} P_k(\xi^{n+1})| \le \frac{M_k}{\|\nabla \bar{\phi}^{n+1}\|^2 + 2}.$$
(2.21)

Therefore, by the fact $\sqrt{A} \le A + 2$ for all $A \ge 0$, we have

$$\|\nabla \phi^{n+1}\| = \eta_k^{n+1} \|\nabla \bar{\phi}^{n+1}\| \le M_k. \quad \Box$$
 (2.22)

2.4. Adaptive time stepping strategy

To fully take advantage of the unconditional stability of our schemes, one should use an adaptive time stepping [28,13,4]. It is clear that ξ^{n+1} should be close to 1 otherwise the numerical solution likely deviates from the exact solution. However, ξ^{n+1} close to 1 can not ensure a good approximation is achieved. Hence we modify the adaptive time-stepping algorithm in [28] as follows. Given a default safety coefficient ρ , a reference tolerance tol, the minimum time steps τ_{max} , a tunable constant r_1 , r_2 and define

$$A_{dp}(e,\tau) = \rho \left(\frac{tol}{e}\right)^{r_1} \tau. \tag{2.23}$$

We update the time step size by the following algorithm:

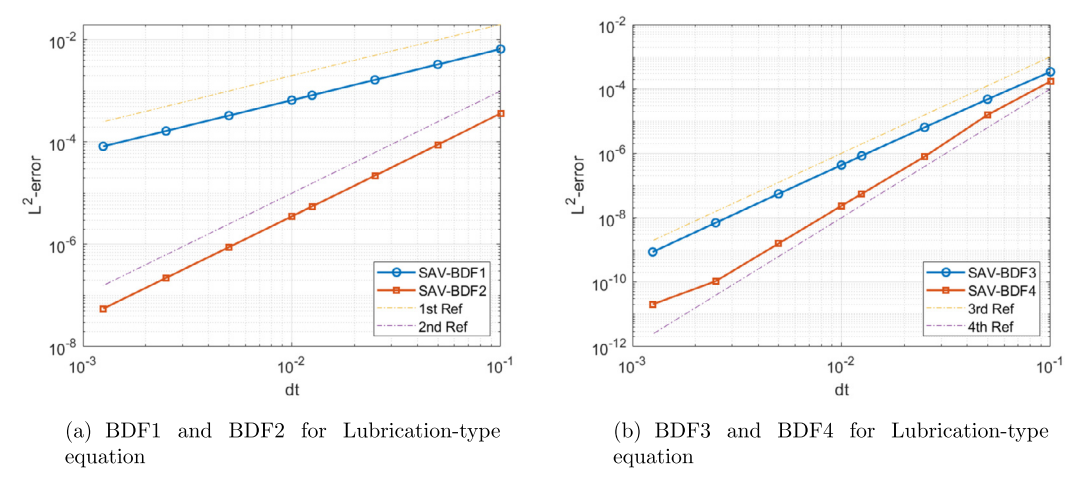


Fig. 1. (Example 1.) Accuracy test for the 1-D Lubrication-type equation using the SAV/BDFk schemes (k = 1, 2, 3, 4).

Algorithm 1: Time step adaptive procedure.

```
Given: the previous time step \tau_n and the previous solutions u^n. step 1. compute u^{n+1} with time step \tau_n; step 2. calculate e_{n+1} = \max\{\|u^{n+1} - u^n\|, r_2|1 - \xi^{n+1}|\}; step 3. if e_{n+1} > tol, then recalculate time step \tau_n \leftarrow \max\{\tau_{\min}, \min\{A_{dp}(e_{n+1}, \tau_n), \tau_{\max}\}\}; goto step 1 step 4. else update time step \tau_{n+1} \leftarrow \max\{\tau_{\min}, \min\{A_{dp}(e_{n+1}, \tau_n), \tau_{\max}\}\}; step 5. endif
```

The above algorithm is only first-order, and is particularly efficient if one is interested only in the steady state solutions. For first-order adaptive schemes, the usual choice of r_1 is 0.5. The choice of r_2 depends on specific problems, and needs to be determined with some trial-and-error process. Higher-order BDF versions can be constructed as in [4,18].

3. Numerical results

In this section, we present ample numerical examples to verify our numerical schemes. For all the examples in this section, periodic boundary conditions are imposed in all directions, and for space discretization, we employ the Fourier-Spectral method [14,25]. We use Nx, Ny and Nz to denote the number of modes in x, y, z directions, respectively.

3.1. Convergence test

We first test accuracy of the two proposed methods.

Example 1 (*Accuracy test of the scheme* (2.3)). We consider the one-dimensional Lubrication-type equation (cf. Case 1 in the introduction) with $f(\phi) = m\phi$. The computational domain is [-1, 1] and the initial condition is

$$\phi(x,0) = \exp(\sin(\pi x)). \tag{3.1}$$

To preserve positivity, we use the function transform

$$\phi = T(u) = \exp(u). \tag{3.2}$$

The parameters are chosen as $\alpha = 1$, m = 0.0001 and Nx = 64. The reference solution is generated by the fourth-order scheme with $\delta t = 0.0002$. We plot in Fig. 1 (a) the L^2 -error of the first- and second-order schemes at $t_n = 1$, and in Fig. 1 (b), the L^2 -error of the third- and fourth-order schemes at $t_n = 1$. Expected convergence rates are observed for all cases.

Note that the mass is exactly conserved only for $\bar{\phi}^{n+1}$, and with an error of order $O(\delta t^{l_k})$ (I_k defined in (2.3e)) for ϕ^{n+1} . We report in Table 1 the mass error of different schemes at $t_n=1$ for $\bar{\phi}^{n+1}$, which verifies that $E^n_{mass}:=|\int_{\Omega}\phi^{n+1}dx-\int_{\Omega}\phi^0dx|$ is of order $O(\delta t^{l_k})$ for the first-, second- and third-order schemes, and the magnitude of mass error for the fourth order scheme is already very small at large δt .

Example 2 (Accuracy test of the scheme (2.14)). We consider the two dimensional Cahn-Hilliard equation with logarithmic potential and constant mobility, i.e. Case 2 in the introduction with $f(\phi) = m$. The computational domain is $[0,2] \times [0,2]$ with the initial condition

Table 1 Mass error test for the 1-D Lubrication-type equation using the SAV/BDFk schemes (k = 1, 2, 3, 4).

	BDF1	BDF2	BDF3	BDF4
δt	E _{mass}	E _{mass}	E _{mass}	E _{mass}
1.00e-1	2.2291e-5	5.5041e-8	3.9037e-8	3.9164e-12
5.00e-2	6.2430e-6	4.2971e-9	3.3633e-9	1.0436e-13
2.50e-2	1.6521e-6	3.0567e-10	2.6184e-10	2.2204e-15
1.25e-2	4.2495e-7	2.0511e-11	1.8758e-11	4.4409e-16
1.00e-2	2.7352e-7	8.5270e-12	7.9203e-12	0
5.00e-3	6.9165e-8	5.4934e-13	5.2847e-13	4.4409e-16
2.50e-3	1.7390e-8	3.5083e-14	3.4195e-15	0
1.25e-3	4.3599e-9	2.6645e-15	2.2204e-15	4.4409e-16

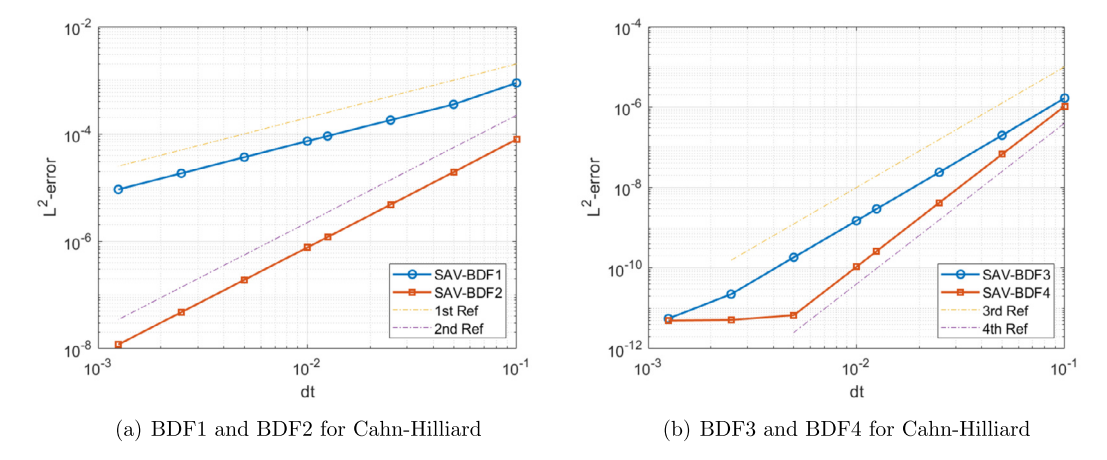


Fig. 2. (Example 2.) Accuracy test for the 2-D Cahn-Hilliard equation using the SAV/BDFk schemes (k = 1, 2, 3, 4).

Table 2 Mass error test for the 2-D Cahn-Hilliard equation using the SAV/BDFk schemes (k = 1, 2, 3, 4).

	BDF1	BDF2	BDF3	BDF4
δt	E _{mass}	E _{mass}	E _{mass}	E _{mass}
1.00e-1	3.0766e-5	6.1988e-11	5.3766e-11	5.6233e-14
5.00e-2	7.9521e-6	4.5424e-12	2.9375e-12	7.2164e-16
2.50e-2	2.0509e-6	3.1247e-13	1.7120e-13	0
1.25e-2	5.0940e-7	2.0539e-14	1.0325e-14	0
1.00e-2	3.2655e-7	8.4377e-15	4.2744e-15	0
5.00e-3	8.1903e-8	4.9960e-16	2.2204e-16	0
2.50e-3	2.0509e-8	1.6653e-16	1.1102e-16	0
1.25e-3	5.1314e-9	0	1.1102e-16	5.5511e-17

$$\phi(x, y, 0) = 0.2 \exp(-\sin^2(\pi x) - \cos^2(\pi y)). \tag{3.3}$$

We use the function transform

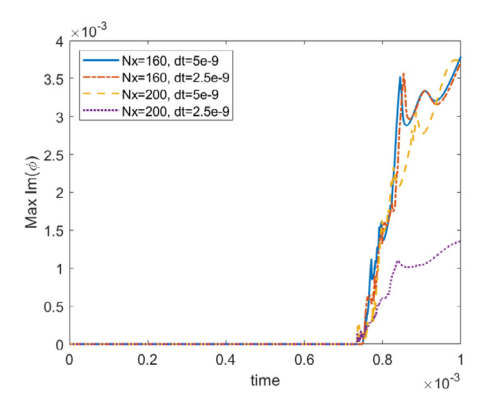
$$\phi = T(u) = \frac{1}{1 + \exp(-u)}. (3.4)$$

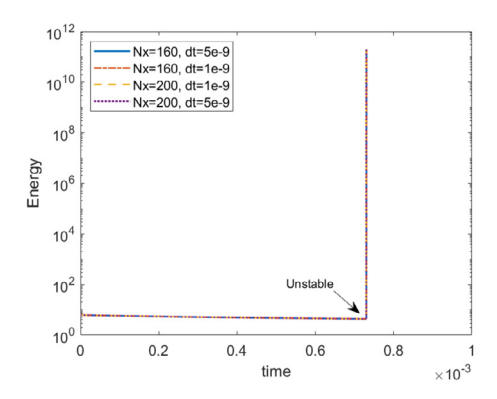
The parameters are chosen as $\alpha=100$, m=0.0001 and Nx=Ny=64. The reference solution is generated by the fourth-order scheme with $\delta t=0.0002$. We plot in Fig. 2 (a) the L^2 -error of the first- and second-order schemes at $t_n=1$, and in Fig. 2 (b), the L^2 -error of the third- and fourth-order schemes at $t_n=1$. Expected convergence rates are observed for all cases. Next, we report in Table 2 the mass error of different schemes at $t_n=1$, which verifies that $E^n_{mass}=O(\delta t^{l_k})$ for large δt and low order schemes, and the magnitude of mass error for high order schemes is very small even for large δt .

3.2. Lubrication-type equation

Example 3. We consider the following one dimensional Lubrication-type equation

$$\phi_t + \partial_x (f(\phi)\partial_x^3 \phi) = 0, \text{ with } f(\phi) = \phi^{1/2}$$
(3.5)





- (a) Maximum value of imaginary part from scheme I: usual semi-implicit scheme
- (b) Energy evolution from Scheme II: function transformation without SAV

Fig. 3. (Example 3.) Failure in solving (3.7) by using Scheme I and Scheme II.

in $\Omega = [-1, 1]$ with the initial condition

$$\phi_0(x) = 0.8 - \cos(\pi x) + 0.25\cos(2\pi x). \tag{3.6}$$

It was shown in [29] that the solution of this problem develops a finite time singularity at $t = t_s$. It was proposed to consider the regularized equation [29]

$$\partial_t \phi_{\varepsilon} + \partial_{x} (f(\phi_{\varepsilon}) \partial_{x}^{3} \phi_{\varepsilon}) = 0 \text{ with } f(\phi_{\varepsilon}) = \frac{\phi_{\varepsilon}^{4} f(\phi_{\varepsilon})}{\varepsilon f(\phi_{\varepsilon}) + \phi_{\varepsilon}^{4}}$$
(3.7)

with $\varepsilon \ll 1$. It was shown in [29] that solution of the regularized problem with any $\varepsilon > 0$ is strictly positive.

In the following, we fix $\varepsilon = 10^{-14}$ and use different time discretization schemes to solve (3.7). Since the problem is nearly singular, we only compare the results using first-order schemes.

• Scheme I. The usual semi-implicit scheme without function transformation: i.e. given ϕ^n , we solve ϕ^{n+1} from

$$\frac{\phi^{n+1} - \phi^n}{\delta t} = \partial_{\chi}(f(\phi^n)\partial_{\chi}\mu^{n+1}),\tag{3.8a}$$

$$\mu^{n+1} = -\partial_x^2 \phi^{n+1}. \tag{3.8b}$$

We set Nx = 160 and $\delta t = 5 \times 10^{-9}$, and plot the maximum value of the imaginary part of the solution in Fig. 3 (a). We observe the imaginary part becomes non zero around the singular time t_s , which means the numerical solution is no longer positive. The situation remains the same even as we use smaller time steps and more spatial modes.

- Scheme II. The semi-implicit scheme with function transformation $\phi = T(u) = \exp(u)$ but without SAV, i.e. we fix $\xi^{n+1} = 1$ in the Scheme 2.3. We set Nx = 160 and $\delta t = 5 \times 10^{-9}$, and plot the energy evolution in Fig. 3 (b). We observe that while the numerical solution remains positive, the scheme becomes unstable at around the singular time t_s . Again, the situation remains the same even we decrease the time step and increase the spatial resolution.
- Scheme III. The semi-implicit scheme with function transformation $\phi = T(u) = \exp(u)$ and with SAV, i.e. the scheme (2.3). We set Nx = 160, $\delta t = 5 \times 10^{-9}$, and plot the minimum value of the numerical solution in Fig. 4 (a) and the SAV factor η in Fig. 4 (b). We observe that the numerical solution approaches zero at around t_s while the SAV factor dips slightly below 1 to allow the scheme to pass the singular time.

The small time step is dictated by the rapid change of energy initially and at around t_s . To overcome this difficulty, we implemented the scheme (2.3) with a time adaptive strategy. We set Nx = 160 and the minimum time step as $\delta t_{min} = 5 \times 10^{-9}$, which is the maximum allowable time step without time step adaptivity. Other parameters for time adaptivity are chosen as $\rho = 0.5$, $r_1 = 0.5$, $r_2 = 1e - 3$, $tol = 10^{-5}$, $\delta t_{max} = 5 \times 10^{-5}$. We plot the solutions at different times in Fig. 5 (a), the energy evolution in Fig. 5 (b), and the time step evolution in Fig. 5 (c). We observe that small time steps were used initially and at around t_s , and the time step gradually increased several magnitudes at later times.

Example 4. We consider the two dimensional Lubrication type equation

$$\phi_t = \nabla \cdot (f(\phi)\nabla \mu) \quad \text{with} \quad f(\phi) = \phi,$$
 (3.9a)

$$\mu = -\Delta\phi,\tag{3.9b}$$

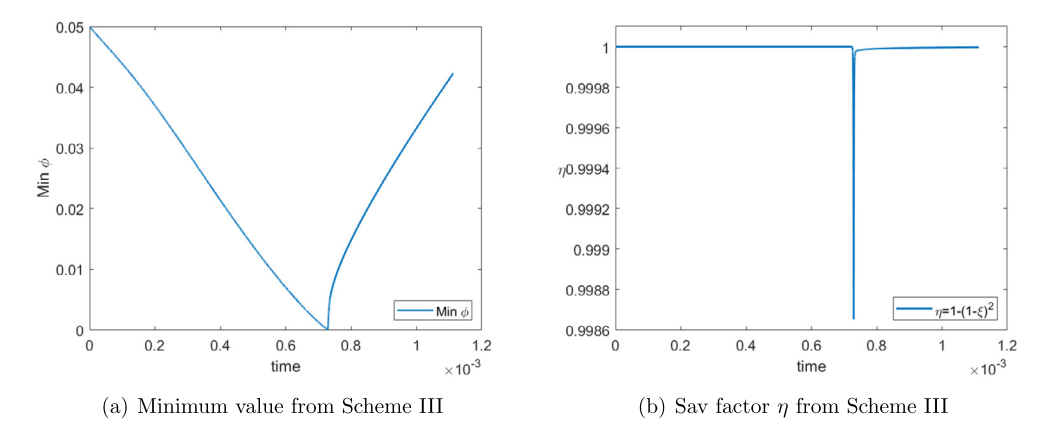


Fig. 4. (Example 3.) Successful computation of (3.7) by using Scheme III: function transformation with SAV.

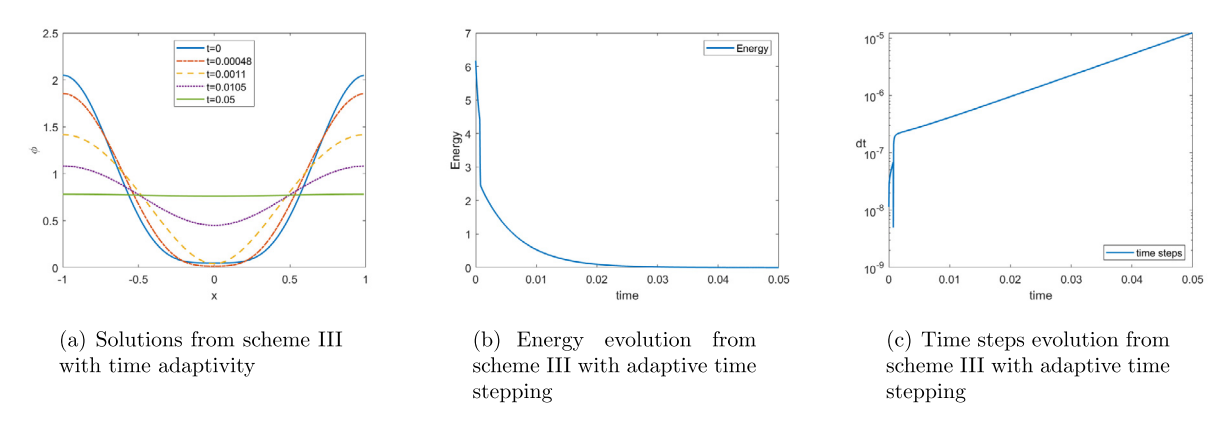


Fig. 5. (Example 3.) Successful computation of (3.7) by using Scheme III with adaptive time stepping.

in $\Omega = [-0.5, 0.5] \times [-1, 1]$ with the initial condition

$$\phi_0(x) = \varepsilon + \frac{\sigma}{40} \exp^{-\sigma(x^2 + y^2)},\tag{3.10}$$

with $\sigma=80$ and $\varepsilon=0.01$. This example was considered in Section 4.1 of [1]. We set Nx=96, Ny=192, and use first-order version of the scheme (2.14) with the function transform $\phi=T(u)=\exp(u)$ and parameters $S_1=2.2$, $S_2=1$ combined with a time adaptive strategy. The parameters for time adaptivity are chosen as $\delta t_{min}=2.5\times 10^{-9}$, $\delta t_{max}=10^{-5}$, $\rho=0.9$, $r_1=0.5$, $r_2=1$, $tol=2\times 10^{-5}$. Fig. 6(a) shows the time evolution of the minimum value of ϕ which are above zero at all times, Fig. 6(b) shows the time evolution of the maximum value of ϕ , and Fig. 6(c) is the time evolution of the total free energy E. We observe that initially, the free energy E decreases very fast, but after around $t=10^{-4}$, the free energy E decreases at a much slower rate. On the other hand, Fig. 6(d) illustrates the time evolution of the adaptive time step δt . We also present in Fig. 7 the instantaneous normalized solution $\phi/max(\phi)$ at the time instants t_1, t_2, t_3, t_4 labeled by the vertical red lines in Fig. 6.

3.3. Cahn-Hilliard equation with logarithmic potential

In this subsection, we consider the two- and three-dimensional Cahn-Hilliard equation with logarithmic potential, i.e. Case 2 in the introduction. We use the same settings as those in [13], namely, $f(\phi) = m\phi(1-\phi)$ in (1.1), and the associated potential is $H(\phi) = \phi \log \phi + (1-\phi) \log(1-\phi) + 3\phi(1-\phi)$ in (1.2), and the initial condition is

$$\phi_0 = \overline{c} + r,\tag{3.11}$$

where \overline{c} is the mean initial condition and r is a random perturbation variable with uniform distribution in [-0.05, 0.05]. All the examples presented in this subsection are computed using the scheme (2.14) with the function transformation $\phi = T(u) = \frac{1}{1+\exp(-u)}$, which not only preserves $\phi \in (0, 1)$, but also lead to simplified nonlinear terms in (2.14), for example:

$$\log(\phi) - \log(1 - \phi) = u,\tag{3.12a}$$

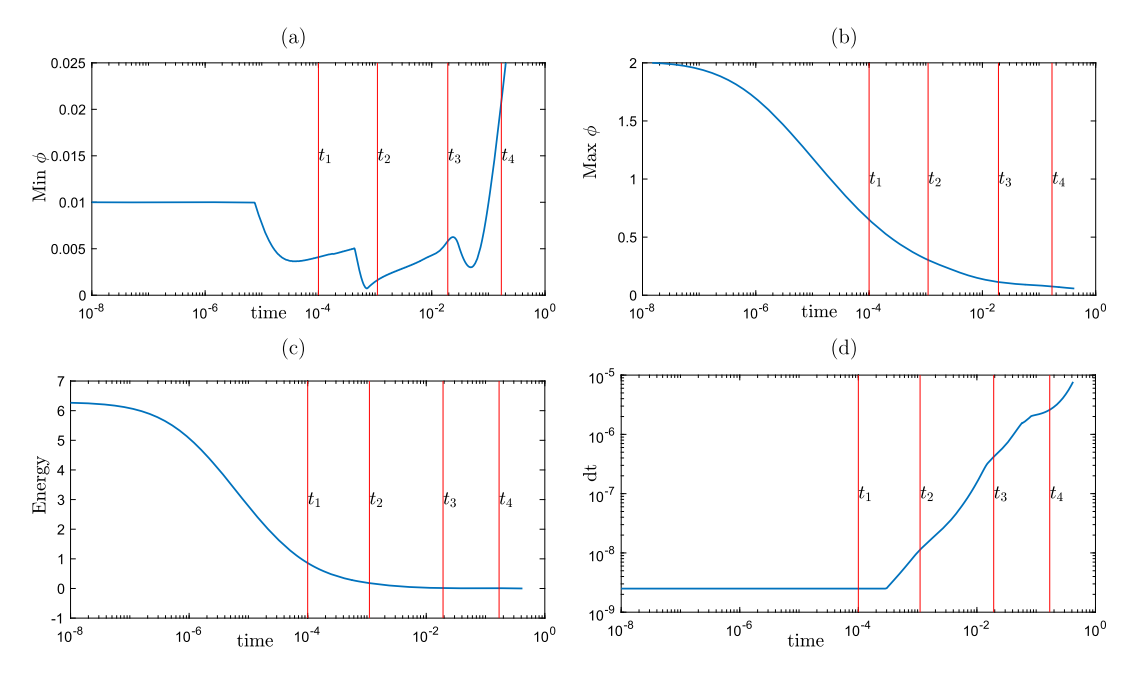


Fig. 6. Example 4. (a) Temporal evolution of the minimum value of ϕ over the entire computational domain; (b) Temporal evolution of the maximum value of ϕ over the entire computational domain; (c) Temporal evolution of free energy E; (d) Temporal evolution of the adaptive time step dt. (For interpretation of the colors in the figure(s), the reader is referred to the web version of this article.)

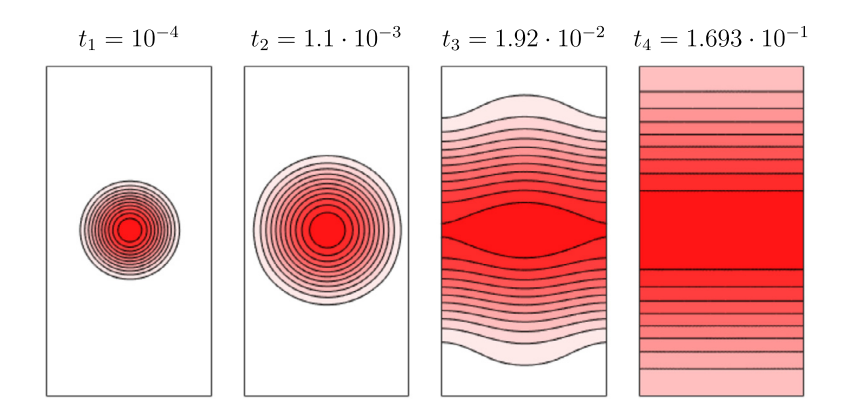


Fig. 7. Example 4. Snapshots of instantaneous normalized $\phi/max(\phi)$ at the time instants as indicated. All the contour levels are equally spaced between 0 to 1, and the colormap is consistent with the contour levels.

$$h(\phi) = h(\phi, u) = u + \lambda - 2\lambda\phi, \tag{3.12b}$$

$$T'(u) = (1 - T(u))T(u) = (1 - \phi)\phi, \tag{3.12c}$$

$$\frac{T''(u)}{T'(u)} = 1 - 2T(u) = 1 - 2\phi. \tag{3.12d}$$

Example 5. In this example, we consider the two dimensional Cahn-Hillard equation in a unit square at two different α values, $\alpha = 3000$ and $\alpha = 6000$ with the mean initial condition $\overline{c} = 0.63$. For both cases, we use the scheme (2.14) with $S_1 = 0.2m$ and $S_2 = 2$. The spatial resolutions used are $N_x = N_y = 128$, time step $dt = 10^{-8}$ for $\alpha = 3000$ and $N_x = N_y = 256$, time step $dt = 2 \times 10^{-9}$ for $\alpha = 6000$. We conduct the simulations using the first order version of (2.14) in order to compare the results obtained using a first order scheme in [13].

Fig. 8(a) and Fig. 8(b) show the time evolution of free energy E at $\alpha = 3000$ and $\alpha = 6000$, respectively. These energy plots are consistent with the corresponding results in Figure 5 and Figure 15 of [13].

In addition, we present in Fig. 9 and Fig. 10 snapshots of the solution at exactly the same time instants as the Figure 6 and Figure 11 in [13], respectively. The dynamical process and the steady states obtained by our scheme are visually comparable with the results presented in [13].

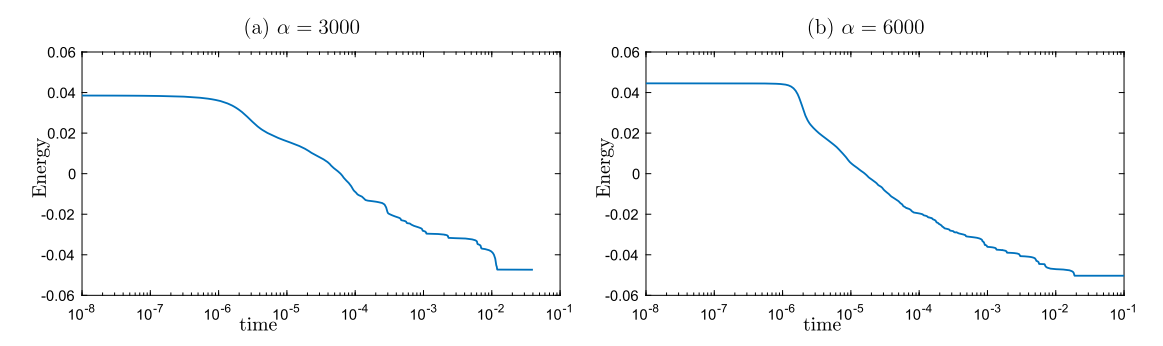


Fig. 8. Example 5. Temporal evolution of free energy at (a) $\alpha=3000$ and (b) $\alpha=6000$. In both cases, the mean initial conditions are $\bar{c}=0.63$.

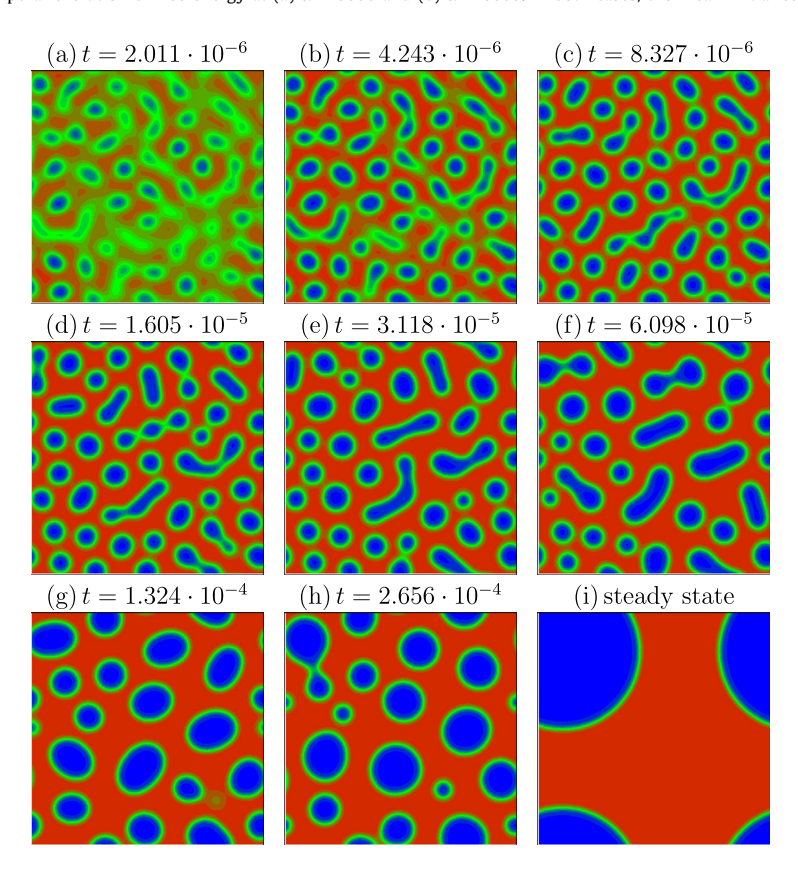


Fig. 9. Example 5. Snapshots of ϕ at different time instants as indicated. The solutions are simulated at $\alpha = 3000$, $f(\phi) = 3000\phi(1 - \phi)$, mean initial condition $\bar{c} = 0.63$, constant time step dt = 1e - 8 and spatial resolution $N_x = N_y = 128$.

Example 6. We consider the three dimensional Chan-Hillaird equation with logarithmic potential in a unit cube with the mobility function $f(\phi) = m\phi(1-\phi)$ and $f(\phi) = m$. We set $S_1 = 0.2m$, $S_2 = 2$ for the variable mobility case and $S_1 = m$, $S_2 = 1$ for the constant mobility case in the scheme (2.14).

We fix $\alpha=m=200$, the mean initial condition $\overline{c}=0.63$, and use Nx=Ny=Nz=96 for both cases. We use the first-order version of (2.14) with adaptive time steps. In both cases, the same parameters are used for time adaptivity: $\delta t_{min}=2\times 10^{-9}$, $\delta t_{max}=10^{-5}$, $\rho=0.2$, $r_1=0.5$, $r_2=1$, $tol=2\times 10^{-4}$.

Fig. 11 shows the energy evolutions for the variable mobility case (a) $f(\phi) = 200\phi(1-\phi)$ and the constant mobility case (b) $f(\phi) = 200$, and the time steps evolutions for the variable case (c) $f(\phi) = 200\phi(1-\phi)$ and the constant mobility case (d) $f(\phi) = 200$. We observe that in both cases the energy decreases monotonically and we can use quite large time steps at a significant part of times.

Fig. 12 illustrates the instantaneous isosurfaces of the numerical solution with variable mobility $f(\phi) = 200\phi(1-\phi)$. The isosurfaces plotted in each single figure are $\phi = 0.45$ (blue), $\phi = 0.5$ (green) and $\phi = 0.55$ (red). We observe that the isosurface $\phi = 0.5$ forms a circular cylinder shape in the steady state. Similarly, we present in Fig. 13 isosurfaces with constant mobility $f(\phi) = 200$. The isosurface $\phi = 0.5$ in steady state is also a circular cylinder. Moreover, since we use

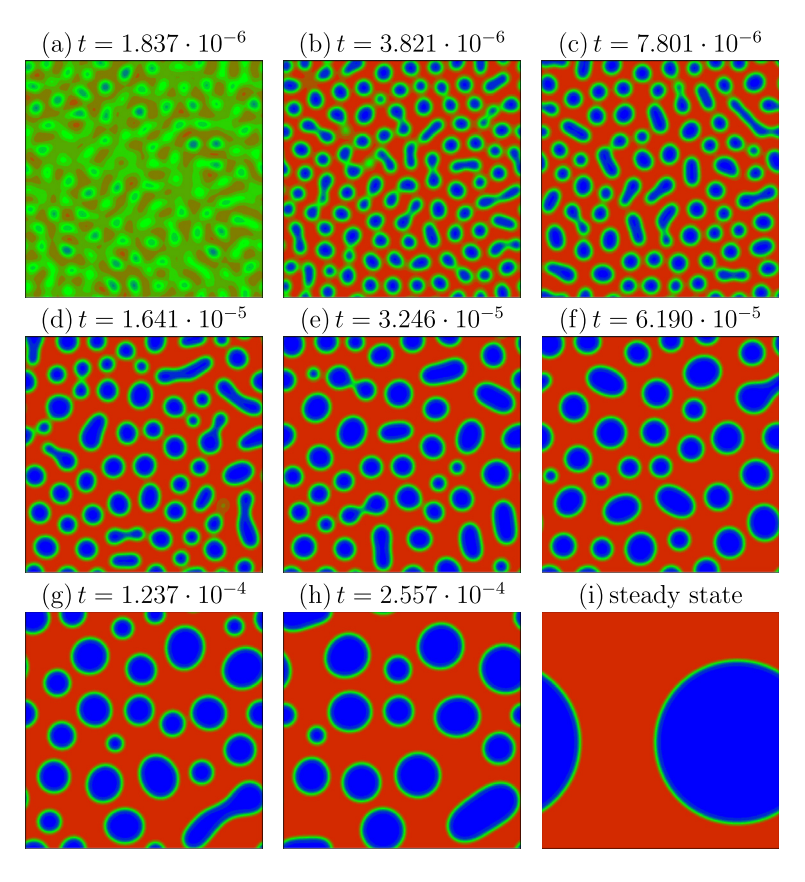


Fig. 10. Example 5. Snapshots of ϕ at different time instants as indicated. The solutions are simulated at $\alpha = 6000$, mobility $f(\phi) = 6000\phi(1-\phi)$, mean initial condition $\bar{c} = 0.63$, constant time step $dt = 2 \times 10^{-9}$ and spatial resolution $N_x = N_y = 256$.

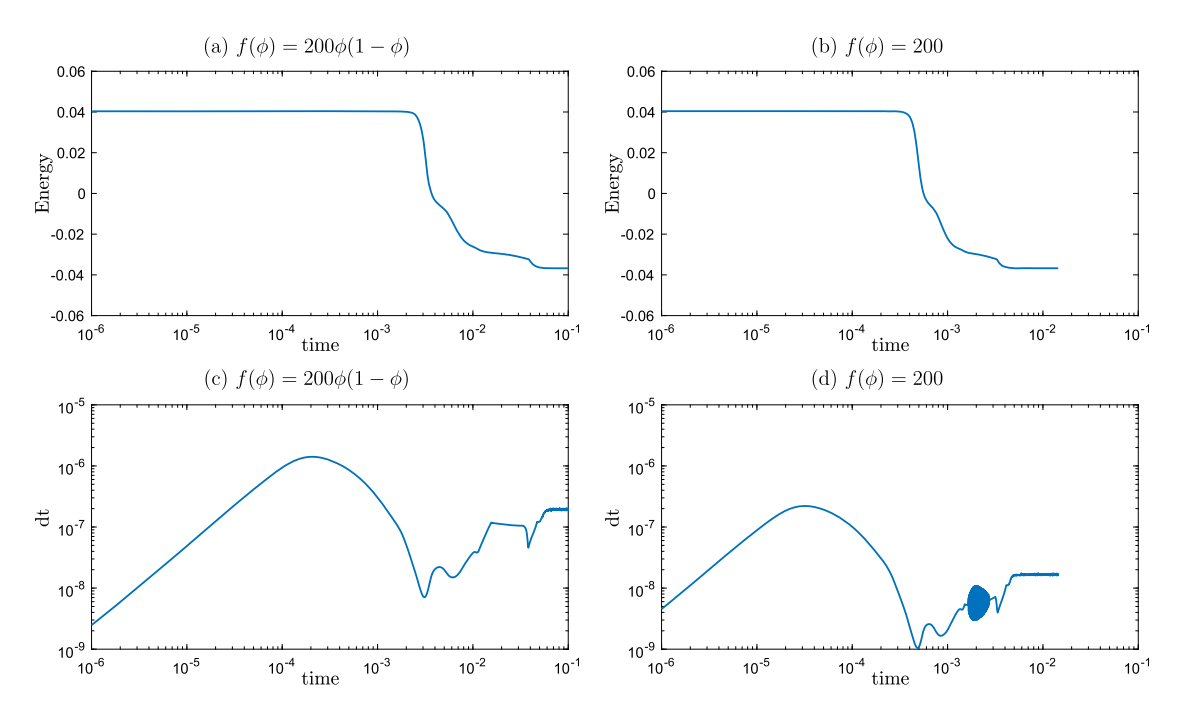


Fig. 11. Example 6. Temporal evolution of free energy E at (a) $f(\phi) = 200\phi(1-\phi)$ and (b) $f(\phi) = 200$; Temporal evolution of the adaptive time steps at (c) $f(\phi) = 200\phi(1-\phi)$ and (d) $f(\phi) = 1$. In both cases, the initial conditions are $\bar{c} = 0.63$, $\alpha = 200$ and spatial resolutions $N_x = N_y = N_z = 96$.

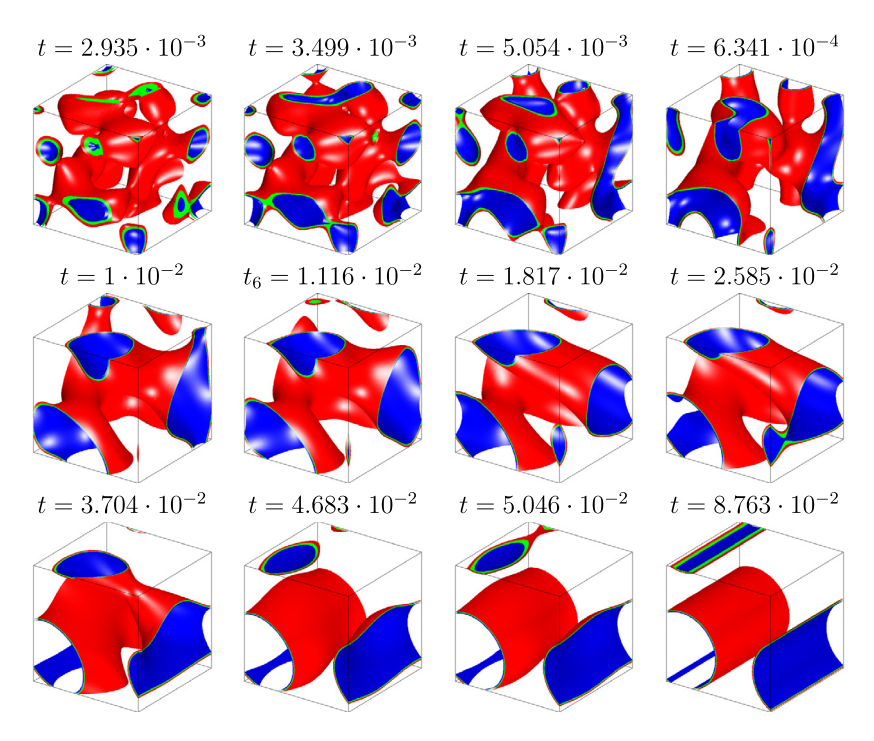


Fig. 12. Example 6. Snapshots of iso-surfaces of ϕ at different time instants as indicated at $\alpha = 200$, mobility $f(\phi) = 200\phi(1-\phi)$ and mean initial condition $\bar{c} = 0.63$. The iso-surfaces are plotted at $\phi = 0.45$ (blue), $\phi = 0.5$ (green) and $\phi = 0.55$ (red).

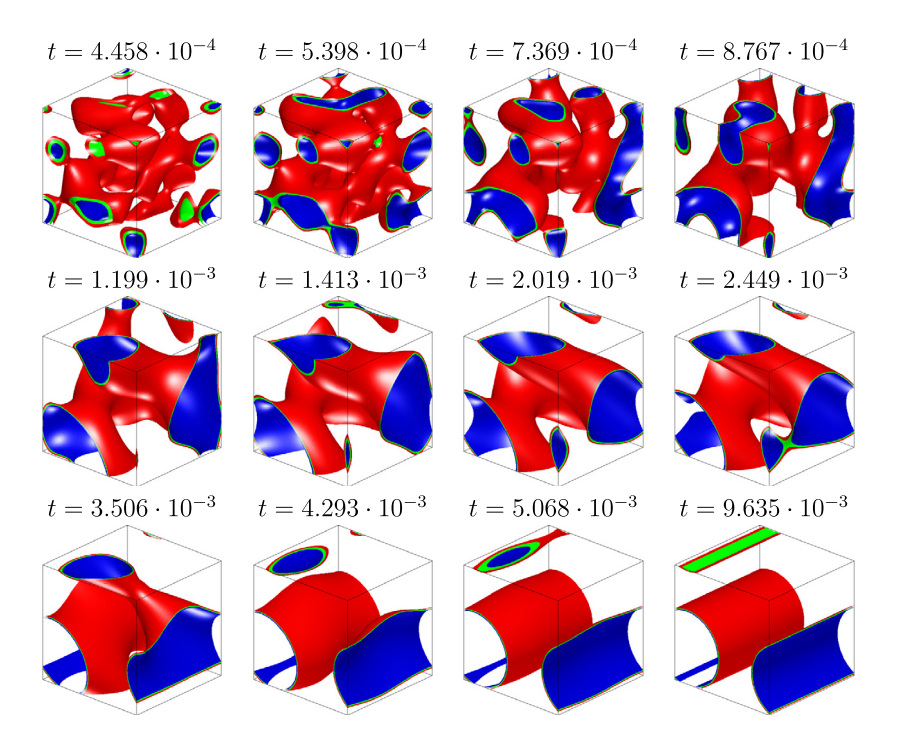


Fig. 13. Example 6. Snapshots of iso-surfaces of ϕ at different time instants as indicated at $\alpha = 200$, mobility $f(\phi) = 200$ and mean initial condition $\bar{c} = 0.63$. The iso-surfaces are plotted at $\phi = 0.45$ (blue), $\phi = 0.5$ (green) and $\phi = 0.55$ (red).

exactly the same initial condition, we observe that the solution with the constant mobility case reaches essentially the same steady state but within a shorter time compared with the variable mobility case.

4. Concluding remarks

We constructed two classes of bound/positivity preserving and unconditionally stable schemes by combining the function transform approach and the SAV approach. The bound/positivity preserving property is ensured by a suitable function transform, while the unconditionally stability is provided with the SAV approach. Both properties are independent of spatial discretizations as long as proper integration by parts is respected, so our time discretization schemes can be combined with any consistent Galerkin type spatial discretization.

The first class of schemes requires solving a coupled second-order linear system with variable coefficients at each time step so it is most suitable for a finite element discretization but can also be used with a finite difference or spectral discretization, while the second class of schemes only requires solving a coupled second-order linear system with constant coefficients so it is particular suitable for a spectral or finite difference discretization in space for which fast solvers may be developed.

Although the transformed equations can be complicated, the second class of schemes is relatively easy to implement as one only needs to solve a coupled second-order linear system with constant coefficients at each time step. On the other hand, the first class of schemes is based on a natural variational approach so it will be relatively easier to carry out a convergence analysis.

We implemented both class of schemes with Fourier-spectral methods for the Lubrication-type equations and the Cahn-Hilliard equations with logarithmic potential, and presented ample numerical examples to validate the accuracy and efficiency of the proposed schemes. It is found that the proposed schemes are able to capture correctly the complex dynamics of the Cahn-Hilliard equations with singular mobility and singular behaviors of the Lubrication-type equations. A drawback of the proposed schemes is that one may need to use smaller time steps compared with a usual approach without function transform. But this is more than offset by their other nice properties, and this situation can be improved by using an adaptive time stepping strategy.

CRediT authorship contribution statement

Fukeng Huang, Jie Shen and Ke Wu all contributed to the conceptualization, methodology and writing. Fukeng Huang and Ke Wu carried out all the numerical simulations.

Declaration of competing interest

The authors declare that they have no known competing financial interests or personal relationships that could have appeared to influence the work reported in this paper.

References

- [1] Andrea L. Bertozzi, Ning Ju, Hsiang-Wei Lu, A biharmonic-modified forward time stepping method for fourth order nonlinear diffusion equations, Discrete Contin. Dvn. Svst. 29 (4) (2011) 1367–1391.
- [2] John W. Cahn, John E. Hilliard, Free energy of a nonuniform system. I. Interfacial free energy, J. Chem. Phys. 28 (2) (1958) 258-267.
- [3] Wenbin Chen, Cheng Wang, Xiaoming Wang, Steven M. Wise, Positivity-preserving, energy stable numerical schemes for the Cahn-Hilliard equation with logarithmic potential, J. Comput. Phys.: X 3 (2019) 100031.
- [4] Wenbin Chen, Xiaoming Wang, Yue Yan, Zhuying Zhang, A second order BDF numerical scheme with variable steps for the Cahn-Hilliard equation, SIAM J. Numer. Anal. 57 (1) (2019) 495–525.
- [5] Qing Cheng, Jie Shen, A new Lagrange multiplier approach for constructing structure preserving schemes, I. Positivity preserving, 2021.
- [6] Qing Cheng, Jie Shen, A new Lagrange multiplier approach for constructing structure-preserving schemes, II. Bound preserving, 2021.
- [7] Lixiu Dong, Cheng Wang, Steven M. Wise, Zhengru Zhang, A positivity-preserving, energy stable scheme for a ternary Cahn-Hilliard system with the singular interfacial parameters, J. Comput. Phys. (2021) 110451.
- [8] Lixiu Dong, Cheng Wang, Hui Zhang, Zhengru Zhang, A positivity-preserving, energy stable and convergent numerical scheme for the Cahn-Hilliard equation with a Flory-Huggins-deGennes energy, Commun. Math. Sci. 17 (4) (2019) 921–939.
- [9] Lixiu Dong, Cheng Wang, Hui Zhang, Zhengru Zhang, A positivity-preserving second-order BDF scheme for the Cahn-Hilliard equation with variable interfacial parameters, Commun. Comput. Phys. 28 (3) (2020) 967–998.
- [10] Jérôme Droniou, Christophe Le Potier, Construction and convergence study of schemes preserving the elliptic local maximum principle, SIAM J. Numer. Anal. 49 (2) (2011) 459–490.
- [11] Qiang Du, Lili Ju, Xiao Li, Zhonghua Qiao, Maximum principle preserving exponential time differencing schemes for the nonlocal Allen–Cahn equation, SIAM J. Numer. Anal. 57 (2) (2019) 875–898.
- [12] Qiang Du, Lili Ju, Xiao Li, Zhonghua Qiao, Maximum bound principles for a class of semilinear parabolic equations and exponential time-differencing schemes, SIAM Rev. 63 (2) (2021) 317–359.
- [13] Héctor Gómez, Victor M. Calo, Yuri Bazilevs, Thomas J.R. Hughes, Isogeometric analysis of the Cahn–Hilliard phase-field model, Comput. Methods Appl. Mech. Eng. 197 (49–50) (2008) 4333–4352.
- [14] D. Gottlieb, S.A. Orszag, Numerical Analysis of Spectral Methods: Theory and Applications, SIAM-CBMS, Philadelphia, 1977.
- [15] Jingwei Hu, Xiaodong Huang, A fully discrete positivity-preserving and energy-dissipative finite difference scheme for Poisson-Nernst-Planck equations, Numer. Math. (2020) 1–39.
- [16] Fukeng Huang, Jie Shen, Bound/positivity preserving and energy stable sav schemes for dissipative systems: applications to Keller-Segel and Poisson-Nernst-Planck equations, SIAM J. Sci. Comput. 43 (3) (2021) A1832–A1857.
- [17] Fukeng Huang, Jie Shen, Implicit-explicit BDF k SAV schemes for general dissipative systems and their error analysis, Comput. Methods Appl. Mech. Eng. 392 (2022) 114718.

- [18] Fukeng Huang, Jie Shen, Zhiguo Yang, A highly efficient and accurate new scalar auxiliary variable approach for gradient flows, SIAM J. Sci. Comput. 42 (4) (2020) A2514–A2536.
- [19] Buyang Li, Jiang Yang, Zhi Zhou, Arbitrarily high-order exponential cut-off methods for preserving maximum principle of parabolic equations, SIAM J. Sci. Comput. 42 (6) (2020) A3957–A3978.
- [20] Hong-lin Liao, Tao Tang, Tao Zhou, A second-order and nonuniform time-stepping maximum-principle preserving scheme for time-fractional Allen-Cahn equations, J. Comput. Phys. 414 (2020) 109473.
- [21] Hailiang Liu, Hui Yu, Maximum-principle-satisfying third order discontinuous Galerkin schemes for Fokker-Planck equations, SIAM J. Sci. Comput. 36 (5) (2014) A2296-A2325.
- [22] Jian-Guo Liu, Li Wang, Zhennan Zhou, Positivity-preserving and asymptotic preserving method for 2D Keller-Segal equations, Math. Comput. 87 (311) (2018) 1165–1189.
- [23] Changna Lu, Weizhang Huang, Erik S. Van Vleck, The cutoff method for the numerical computation of nonnegative solutions of parabolic PDEs with application to anisotropic diffusion and lubrication-type equations, J. Comput. Phys. 242 (2013) 24–36.
- [24] Partho Neogi, C.A. Miller, Spreading kinetics of a drop on a smooth solid surface, J. Colloid Interface Sci. 86 (2) (1982) 525-538.
- [25] Jie Shen, Tao Tang, Li-Lian Wang, Spectral Methods: Algorithms, Analysis and Applications, vol. 41, Springer Science & Business Media, 2011.
- [26] Xiangxiong Zhang, Chi-Wang Shu, On positivity-preserving high order discontinuous Galerkin schemes for compressible Euler equations on rectangular meshes, J. Comput. Phys. 229 (23) (2010) 8918–8934.
- [27] Xiangxiong Zhang, Chi-Wang Shu, Maximum-principle-satisfying and positivity-preserving high-order schemes for conservation laws: survey and new developments, Proc. R. Soc. A, Math. Phys. Eng. Sci. 467 (2134) (2011) 2752–2776.
- [28] Zhengru Zhang, Zhonghua Qiao, An adaptive time-stepping strategy for the Cahn-Hilliard equation, Commun. Comput. Phys. 11 (4) (2012) 1261–1278.
- [29] Liya Zhornitskaya, Andrea L. Bertozzi, Positivity-preserving numerical schemes for lubrication-type equations, SIAM J. Numer. Anal. 37 (2) (2000) 523–555.
- [30] J. Zhu, L.Q. Chen, Jie Shen, V. Tikare, Microstructure dependence of diffusional transport, Comput. Mater. Sci. 20 (2001) 37-47.